



Original Article

Application of 2D electrical resistivity tomography to engineering projects: Three case studies

Rungroj Arjwech^{1*} and Mark E. Everett²

¹ *Department of Geotechnology, Faculty of Technology,
Khon Kaen University, Mueang, Khon Kaen, 40002 Thailand.*

² *Department of Geology and Geophysics,
Texas A&M University, College Station, Texas.*

Received: 2 December 2014; Accepted: 1 July 2015

Abstract

Electrical resistivity tomography (ERT) is a non-invasive geophysical method of primary interest for addressing subsurface engineering problems. The method is based on the assumption that subsurface geological materials have significant resistivity contrasts that can be identified based on measurements on the surface. This paper presents three different case studies that have been carried out at different sites. The first case study visualizes the contrast between high resistivity zones of hard bedrocks and low resistivity zones of weathered rocks. Similar to the first case study, the second case study shows high resistivity contrasts that clearly distinguishes the shape of a footing located within the surrounding materials. The third case study shows no clear low resistivity zone that can be identified as a leaking zone. The 2D ERT survey method used in these three investigations has been shown to be useful as a cost-effective and rapid method to obtain wide area subsurface information that is relevant for subsurface engineering problems.

Keywords: non-invasive geophysical methods, electrical resistivity tomography (ERT), unknown bridge foundation determination, seepage

1. Introduction

Geophysics involves the use of non-invasive techniques to determine subsurface anomalies without having to engage in destructive excavation (Barker, 1993). Non-destructive testing (NDT) is defined as the evaluation of the properties of a material, component or system without causing damage (Louis, 1995). In the last few decades, geophysical NDT methods have been developed and increasingly applied for addressing engineering problems. As one example, transportation personnel have used geophysical NDT methods in assisting geotechnical site investigation, construction, and

maintenance of highways (Dahlin, 2001; Wightman and Jalinoos, 2003). In many instances, geophysical NDT methods enhance the reliability and speed, and also reduce the cost of a geotechnical investigation (Anderson *et al.*, 2008). Assessing and characterizing geotechnical conditions can become complex and costly in the presence of obstacles such as difficult access, irregular terrain and ground conditions, or regulatory constraints. Results based on traditional methods such as penetration testing or direct sampling may be of limited utility. Surface geophysical techniques can provide alternate, wide-area methods for subsurface characterization and information regarding relevant material properties (Rucker, 2006). Though geophysics is not a substitute for geotechnical boring or testing, it is often a very cost-effective and efficient means of constructing contiguous 2D and 3D images of the subsurface and determining in-situ bulk properties (Anderson *et al.*, 2008).

* Corresponding author.
Email address: rungroj@kku.ac.th

The electrical resistivity tomography (ERT) method is one of the most widely used near-surface geophysical survey methods for civil engineering applications (Castilho and Maia, 2008). The method has been used for mapping electrical resistivity in two and three dimensions (Dahlin, 2001). Previous studies have demonstrated the use of the ERT method for identification of bedrock structures (Hsu *et al.*, 2010; Chambers *et al.*, 2013), cavities or sinkholes (Kaufmann *et al.*, 2012; Gómez-Ortiz and Martín-Crespo, 2012), geotechnical site investigation (Al-Fares W., 2011; Haile and Atsbaha, 2014), slope stability investigation (Marescot *et al.*, 2008; Perrone *et al.*, 2014), and unknown bridge foundation determination (Arjwech *et al.*, 2013; Tucker *et al.*, 2014).

The ERT method may be used for various other purposes in subsurface engineering investigations. This paper aims to further demonstrate the application of the ERT technique on a number of engineering problems. More specifically, the paper presents the results of 2D ERT that have been carried out by the authors in various projects including investigating the subsurface geology of a building construction site, determining the depth of an unknown bridge foundation, and determining seepage from the earthen embankments of a wastewater treatment pond system.

2. Electrical Resistivity Survey

The electrical resistivity technique is based on the assumption that subsurface geological materials exhibit a wide variability of resistivity values and that geological boundaries can be identified based on measurements of resistivity. If a target of interest has a sufficiently large electrical resistivity contrast with respect to that of the surrounding material, it can be detected by surface measurements of voltage following the injection of current through pairs of electrodes (Barker, 1993).

The purpose of a resistivity survey is thus to determine the distribution of underground resistivity from measurements of potential difference, or voltage, made on the ground surface. An electric current I (amperes, A) is injected at electrode C_1 and withdrawn at electrode C_2 as shown in Figure 1, while two other electrodes P_1 and P_2 are used to record the resulting potential difference ΔV (volt, V),

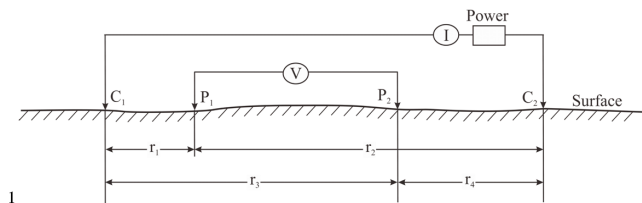


Figure 1. Two current (C_1 and C_2) and two potential (P_1 and P_2) electrodes in the standard configuration (Telford *et al.*, 1990).

$$\nabla V = \frac{I\rho}{2\pi} \left\{ \left(\frac{1}{r_1} - \frac{1}{r_2} \right) - \left(\frac{1}{r_3} - \frac{1}{r_4} \right) \right\}, \quad (1)$$

where r is resistivity, while r_1 , r_2 , r_3 , and r_4 are distances of the potential electrodes P_1 and P_2 from the current electrodes C_1 and C_2 , respectively. Equation 1 is valid if the ground has homogeneous resistivity.

In case of inhomogeneous ground, an apparent resistivity r_a is calculated from the relationship between the applied current and the potential difference for a particular electrode arrangement and spacing. It is defined by,

$$\rho_a = \frac{k\Delta V}{I}, \quad (2)$$

where k is a geometric factor dependent on the electrode spacing,

$$k = \frac{2\pi}{\left\{ \left(\frac{1}{r_1} - \frac{1}{r_2} \right) - \left(\frac{1}{r_3} - \frac{1}{r_4} \right) \right\}}. \quad (3)$$

The apparent resistivity clearly depends on the geometry of the electrode configuration. The best electrode configuration for a field survey depends on the sensitivity of the resistivity meter, the background noise level, and the relative importance assigned by the geophysicist to depth of penetration and lateral resolution. Standard electrode configurations used for 2D ERT surveys are Wenner, dipole-dipole, Wenner-Schlumberger, pole-pole, pole-dipole, and equatorial dipole-dipole (Telford *et al.*, 1990; Loke, 2000; Kearey and Brooks, 2002; Dahlin and Zhou, 2004; Loke and Lane, 2004; Loke, 2010).

3. 2D Electrical Resistivity Tomography

A 2D multi-electrode ERT survey may be carried out using a large number of electrodes connected to a multi-core cable. The electrode cable is typically divided into sections of manageable length, which are then connected end-to-end. Electrodes connected to the cable take-outs are inserted into the ground at a specified regular interval along a survey line. A resistivity meter and electronic switching unit are used in conjunction with a user-programmed protocol to automatically measure r_a in a pre-defined sequence of combinations of four electrodes.

Efficient data acquisition is achieved by measuring several voltages simultaneously across multiple pairs of electrodes following a single injection of electric current (Loke, 2000; Bernard, 2003; Hiltunen and Roth, 2003; Loke, 2010). Figure 2 shows an example of electrode arrangement and measurement sequence for a 2D ERT survey. When the data acquisition is completed, data analysis is performed using the RES2DINV (Loke, 2004) software, including 2D pseudo-section plotting, and inversion. The RES2DINV

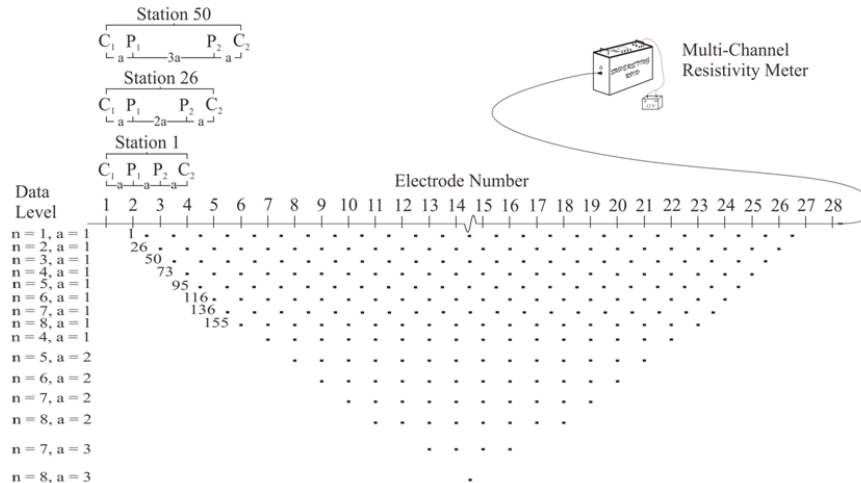


Figure 2. Arrangement of electrodes for a 2D survey and the sequence of measurements used to build up an apparent resistivity pseudo-section (Loke, 2000).

inversion algorithm is described by Loke and Barker (1995; 1996) and Yang (1999) and is based on a smoothness-constrained least squares approach (DeGroot-Hedlin and Constable, 1990).

4. 2D ERT to Investigate Subsurface Geology at a Building Construction Site

4.1 Site description

A nine-story building is planned to be constructed on a site that is situated on a ridge characterized by cuesta topography aligned East-West (Figure 3A). The terrain is covered with trees and bushes, with numerous boulders and bedrock also contributing to make access difficult for a resistivity survey. The bedrock is well exposed on the surface and delineates the rim of a sedimentary basin structure.

4.2 Methods

The objective of this study is to identify bedrock. ERT data acquisition comprises six profiles (ChRU 1-6) using SYSCAL R1 Plus by IRIS Instrument. Hybrid Wenner-Schlumberger electrode array configurations were selected with 5 m electrode spacing, yielding a total length of each profile of 235 m. In order to cover the entire proposed site using only a few ERT profiles, the first two profiles were separated by 17.5 m and oriented East-West, whereas the other four profiles were separated by 20 m intervals and oriented North-South (Figure 3D).

4.3 Interpretation

The inversion results indicate that good resistivity data were acquired, converged with a RMS misfit of lower than 7 at the maximum fifth iteration. The profiles ChRU1 and

2 show similar resistive zones and thicknesses (Figure 4). The prominent low-resistivity zone of $<100 \Omega\text{m}$ in the near-surface towards the west corresponds to location without exposed bedrock and hence is interpreted as a zone of weathered rock and top-soil. The high-resistivity zone $>200 \Omega\text{m}$ that is dominant at the east end of the profiles is interpreted as sandstone bedrock.

The inversion results from the profiles ChRU3 and 4 show near-surface high resistivity $>200 \Omega\text{m}$ which is consistent with resistant sandstone bedrock exposed on the surface. The high resistivity zone thins toward the north and extends to a maximum of ~ 15 m in depth at the southern ends of the profiles. A low resistivity zone close to the northern ends can be seen at lower depths in both sections. These lower zones of resistivity $<100 \Omega\text{m}$ are the ones imaged on the orthogonal profiles ChRU1 and 2. The inversion results of the profiles ChRU5 and 6 show similar structures as found in profiles ChRU3 and 4 but thicker high-resistivity zones are evident.

4.4 Data verification

Due to a lack of well log and other subsurface data, the resistivity images were verified by comparing against available geological information nearby the site. A sandstone outcrop is well exposed on the front slope in Figure 5 and reveals clear stratification. The lithology consists of alternating beds of hard well-lithified sandstone overlying highly weathered sandstone and siltstone with a distinctive sharp, erosive, and conformable contact. The zone of high resistivity $>200 \Omega\text{m}$ in Figure 4 is interpreted to be caused by the resistant bed of sandstone, whereas the zone of lower resistivity $<200 \Omega\text{m}$ is interpreted to be caused by the weathered sandstone and siltstone. The construction activities planned for the site can take advantage of the subsurface information that is provided by these ERT results.



Figure 3. View of (A) the cuesta topography of the study area; views (B and C) along survey profiles illustrating the complex terrain consisting of large boulders and bedrocks on the surface; schematic plan view of location of the resistivity profiles ChRU1-6 (D).

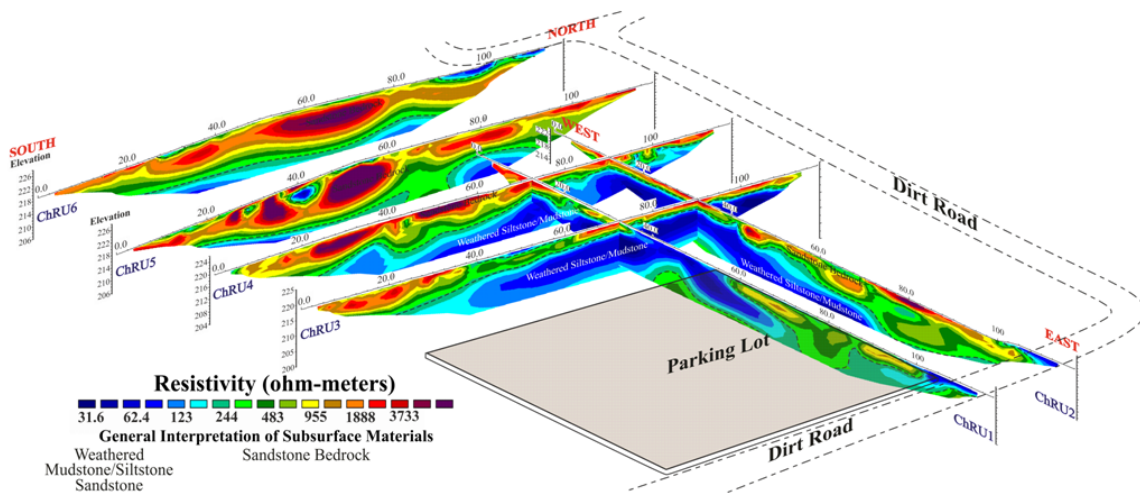


Figure 4. Resistivity fence diagram from all inversion images shows subsurface features of the construction site study area. Red and green colors correspond to high resistivity, whereas blue is low resistivity.

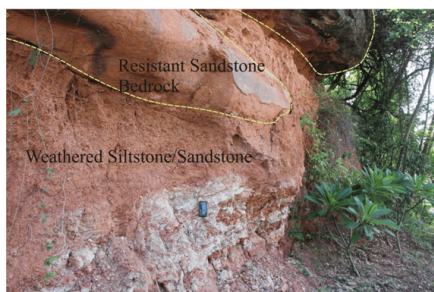


Figure 5. Mapping of the geology from an outcrop study near the construction site shows a resistant sandstone bed on the top, overlying weathered sandstone and siltstone, with a sharp contact between the two units.

5. 2D ERT for Unknown Bridge Foundation Depth Determination

5.1 Site description

A railway bridge built across a river has been identified as containing unknown foundations due to non-existent information about their design and construction. A representative foundation located on the steep slope of the river bank is difficult to characterize using traditional exploratory methods. For example, the water level rises and floods part of the foundation during the rainy season. The foundation has hexagonal cross-sectional shape with 8, 3, and 3 m side lengths (Figure 6).

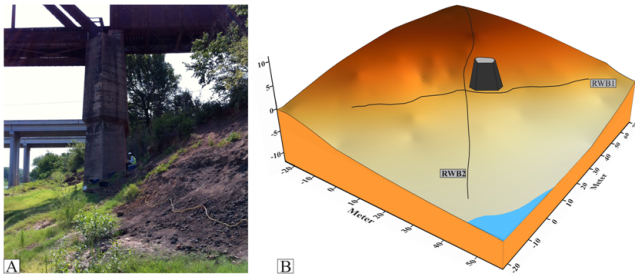


Figure 6. ERT profile RWB1 was aligned parallel to the river (A); a 3D schematic view of the railway bridge site showing resistivity survey profile and location of the hexagonal foundation (B).

5.2 Methods

Unknown bridge foundations pose a significant safety risk due to the possibility of their undermining by stream scour and erosion. So the objective of this study is to visualize unknown foundation shape and depth. A 2D ERT data set was collected for this study using the SuperSting™ R8/IP system by Advanced Geosciences Inc., (AGI). The survey consisted of two orthogonal profiles (RWB1-2) conducted with dipole-dipole electrode configurations of 28-electrodes at 2 m spacing. The total length of each survey profile is thus 54 m. This layout provides the capability to map the narrow vertical subsurface foundation. The profiles passed within 0.5 m alongside the foundation and were laid out parallel and perpendicular to the river, respectively. The profiles intersected near one corner of the foundation, as shown in the Figure 6.

5.3 Interpretation

Both (RWB1-2) inversions converged with a RMS misfit of lower than 4 after five iterations. The results indicate a strong contrast between the resistivity of the foundation and that of the surrounding geological materials, as shown in Figure 7. The ERT images generally show lower resistivity zones corresponding to geological materials and a central higher resistivity zone corresponding to the concrete foundation itself. The zones of low resistivity extend to both end sections of the profile where clay particles and elevated moisture act to increase electrical conductivity. The shallowest exposed bedrock is found close to the foundation, with resistivity values ranging between 10-40 Ωm. This layer represents weathered to moderately weathered shale, as observed on the surface. A high resistivity anomaly >80 Ωm coincides with the concrete foundation. Its shape is somewhat rectangular, being 11x5 m for RWB1 and 3x5 m for RWB2, respectively and a depth of 5 m. This zone is interpreted to be the resistivity signature of a large spread footing.

5.4 Data verification

Both resistivity images at the railway bridge site show that the horizontal size of the anomaly associated with the spread footing is consistent with the actual size of the foundation (11x3 m wide). A bridge layout plan showing the designed depth of the footing is not available so the ERT-interpreted foundation depth could not be verified. Without confirmation documentation provided by the original layout plans, acquiring two surveys conducted on perpendicular profiles increases the reliability relative to that provided by a single profile in any direction.

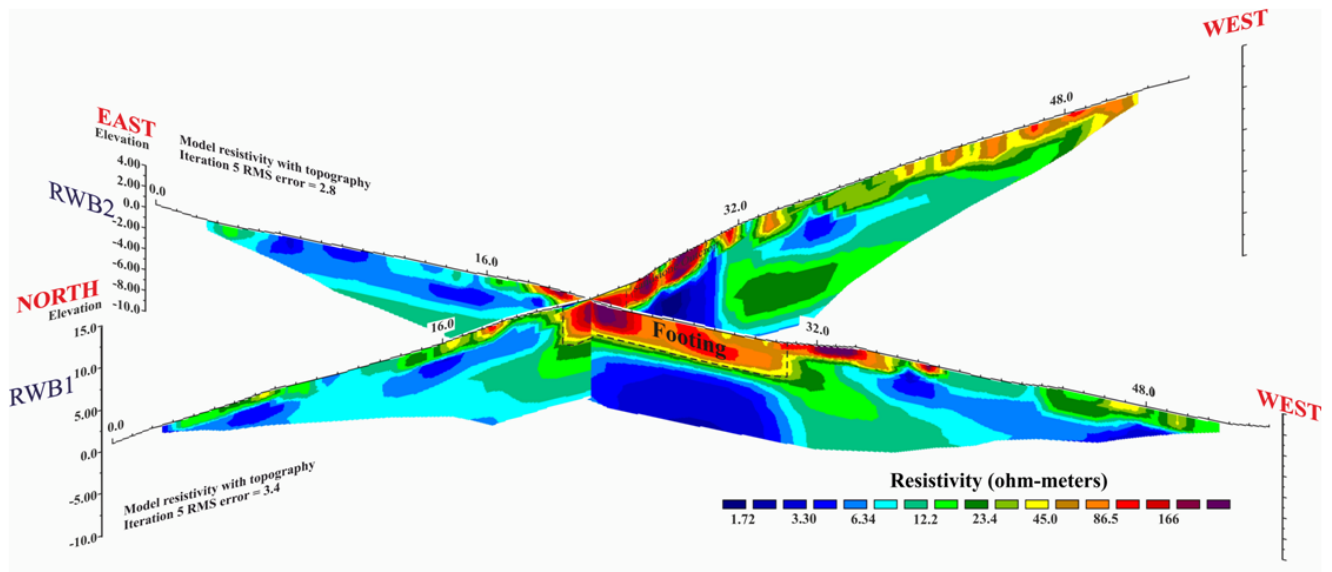


Figure 7. Inversion results at the railway bridge clearly show a high resistivity zone interpreted as a shallow footing at about the midpoint of the survey profiles.

Generally, the 2D ERT method for foundation determination is somewhat straightforward to interpret due to the known location of the foundation along the profile. A detailed interpretation is usually done by qualitative comparison of the observed surface location with that inferred on the specific inversion image. The depth of the foundation can then be directly visualized on the inversion result. In other types of engineering problems, the horizontal location of the target may not be known in advance.

6. 2D ERT for Determining Seepage of Earthen Embankments of a Wastewater Treatment Pond System

6.1 Site description

A wastewater treatment pond system is constructed on Quaternary loess deposits. The pond system consists of multiple ponds in series (Figure 8). The concern of seepage through the earthen embankments is rising because loess is easily erodible and collapsible. Dry loess usually has high shearing resistance; however when wet it loses considerable shear strength (Phien-wej *et al.*, 1991).

6.2 Methods

The objective of this study is to image the possibility of seepage zone. Two 2D ERT profiles (WTPS1-2) were acquired along the west and south sides of the pond system using SYSCAL R1 Plus by IRIS Instruments. Possible seepage is located on these sides because groundwater flow along the hydraulic gradient intersects them. The ERT survey profiles were deployed atop the earthen embankments using hybrid Wenner-Schlumberger electrode configurations with 48 electrodes and 5 m spacing. An additional “roll along” technique was adopted to extend of the length of each survey profile. The length of WTPS1 is 445 m and WTPS2 is 390 m.

The two survey profiles intersected at the southwest corner of the pond system.

6.3 Interpretation

The inversion results were converged to a maximum of 5% of RMS error in five iterations, as shown in Figure 9. A low resistivity zone of < 20 Wm on profile WTPS1 is evident at three distinct locations between distances 280-320 m near the surface on the downstream side. These zones are attributed to the effect of water running through known drainage systems. The resistivity anomalies are consistent with their locations on the surface where the treated water is drained. However the low resistivity zones are distorted compared to the actual shape of the drains as expected for geophysical imaging. The two inversion images show no other signs of low resistivity zone identified as seepage anomaly. A low resistivity level located below 15 m is clearly seen. This zone is interpreted as the underlying groundwater level.

7. Conclusions

The concern of geotechnical engineers about uncertainties in ground conditions suggests the utilization of 2D



Figure 8. ERT profile WTPS2 was aligned North-South (A); schematic plan view of wastewater treatment pond systems showing orthogonal resistivity survey profiles (B).

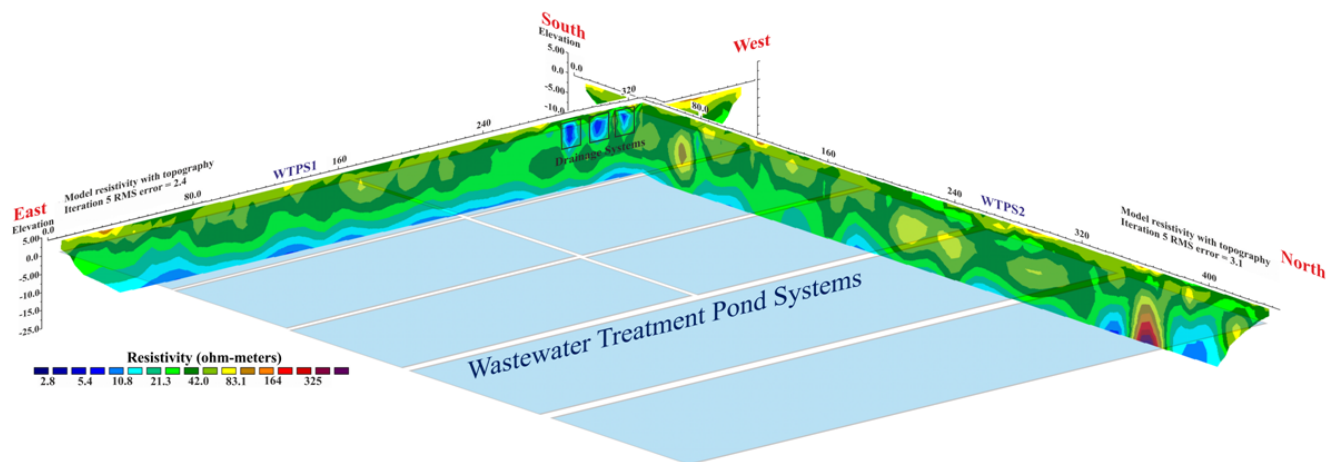


Figure 9. Inversion images show no indication seepage. The low resistivity zones are interpreted as drainage systems that are consistent with their known locations on surface.

ERT for characterizing the subsurface. The three case studies presented herein demonstrate the successful use of 2D ERT. The first study showed that ERT can be used for planning building construction, as it is a technique that can discriminate between resistant and weathered bedrocks. ERT is also seen to be an effective tool for imaging the depth of large-shallow bridge foundations. Finally, ERT can be used effectively to determine whether there is seepage through earthen embankments of wastewater treatment pond systems.

The 2D ERT method used in these three investigations is as a cost-effective and rapid means to obtain wide area subsurface information. Though 2D ERT is not a substitute for geotechnical boring or testing, it is a non-invasive technique, combining rapid acquisition, and safe operation. The equipment is portable and setup can often be effectively deployed over densely vegetated or steep slope areas that might not be easily accessible to traditional invasive methods. The ERT results provide 2D subsurface images with good spatial resolution along the survey profile. Based on the experience gained by applications such as three case studies presented herein, it is recommended that the 2D ERT method should be increasingly used by geotechnical engineers. Moreover, other complementary geophysical methods can be used in an integrated exploration that may be able to enhance images of subsurface geological materials over images obtained using the ERT method alone.

Acknowledgements

We gratefully acknowledge the Texas Department of Transportation, Texas, U.S.A. and the Department of Geotechnology, Khon Kaen University, Thailand, for support and encouragement.

References

- Al-Fares, W. 2011. Contribution of the geophysical methods in characterizing the water leakage in Afamia B dam, Syria. *Journal of Applied Geophysics*. 75, 464-471.
- Anderson, N., Hoover, R. and Sirles, P. 2008. Geophysical methods commonly employed for geotechnical site characterization. *Transportation Research Broad of the National Academies*.
- Arjwech, R., Everett, M., Briaud, J.L., Hurlbauss, S., Medina-Cetina, Z., Tucker, S. and Yosefpour, N. 2013. Electrical resistivity imaging of unknown bridge foundations. *Near Surface Geophysics*. 11, 591-598.
- Barker, P. 1993. *Techniques of archaeological excavation*. Taylor and Francis e-Library.
- Bernard, J. 2003. The depth of investigation of electrical methods. IRIS-instruments, France.
- Castilho, G. and Maia, D. 2008. A successful mixed land underwater 3D resistivity survey in an extremely challenging environment in Amazônia. 21th EEGS Symposium on the Application of Geophysics to Engineering and Environmental Problems. 1150-1158.
- Chambers, J.E., Wilkinson, P.B., Wardrop, D., Hameed, A., Hill, I., Jeffrey, C., Loke, M.H., Meldrum, P.I., Kuras, O., Cave, M. and Gunn, D.A. 2012. Bedrock detection beneath river terrace deposits using 3D electrical resistivity tomography. *Geomorphology*. 177-178, 17-25.
- Dahlin, T. 2001. The development of dc resistivity imaging techniques. *Computers and Geosciences*. 27, 1019-1029.
- Dahlin, T. and Zhou, B. 2004. A numerical comparison of 2D resistivity imaging with 10 electrode arrays. *Geophysical Prospecting*. 52, 379-398.
- DeGroot-Hedlin, C. and Constable, S. 1990. Occam's inversion to generate smooth, Two-dimensional models from magnetotelluric data. *Geophysics*. 55, 1613-1624.
- Gómez-Ortiz, D. and Martín-Crespo, T. 2012. Assessing the risk of subsidence of a sinkhole collapse using ground penetrating radar and electrical resistivity tomography. *Engineering Geology*. 149-150, 1-12.
- Haile, T. and Atsbaha, S. 2014. Electrical resistivity tomography, VES and magnetic surveys for dam site characterization, Wukro, Northern Ethiopia. *Journal of African Earth Sciences*. 97, 67-77.
- Hiltunen, D. and Roth, M. 2003. Investigation of bridge foundation sites in karst terrain via multi-electrode electrical resistivity, *Proceeding of the 3rd International Conference on Applied Geophysics – Geophysics*, 2003.
- Hsu, H., Yanites, B., Chen, C. and Chen, Y. 2010. Bedrock detection using 2D electrical resistivity imaging along the Peikang River, central Taiwan. *Geomorphology*. 114, 406-414.
- Kaufmann, O., Deceuster, J. and Quinif, Y. 2012. An electrical resistivity imaging-based strategy to enable site-scale planning over covered palaeokarst features in the Tournaisis area (Belgium). *Engineering Geology*. 133-134, 49-65.
- Kearey, P. and Brooks, M. 2002. *An Introduction to Geophysical Exploration*, Blackwell Science Publications, U.S.A.
- Loke, M.H. and Baker, R.D. 1995. Least-square deconvolution of apparent resistivity pseudosections. *Geophysics*. 60, 1682-1690.
- Loke, M.H. and Barker, R.D. 1996. Practical techniques for 3D resistivity surveys and data inversion. *Geophysical Prospecting*. 44, 499-523.
- Loke, M.H. 2000. *Electrical Imaging s Surveys for Environmental and Engineering Studies, a practical guide to 2-d and 3-d surveys*. Penang, Malaysia.
- Loke, M.H. 2004. RES2DINV ver. 2.14, Geotomo Software Sdn Bsd, Malaysia.
- Loke, M.H. and Lane, J.W. 2004. Inversion of data from electrical resistivity imaging surveys in water covered areas. *Exploration Geophysics*. 35, 266-271.
- Loke, M.H. 2010. 2D and 3D Electric Imaging Surveys, Geotomo Software Sdn Bsd, Malaysia.

- Louis, C. 1995. *Nondestructive Testing; radiography, ultrasonics, liquid penetrant, magnetic particle, eddy current*, ASM International. Materials Park, Ohio, U.S.A.
- Marescot, L., Régis, M. and Chapellier, D. 2008. Resistivity and induced polarization surveys for slope instability studies in the Swiss Alps. *Engineering Geology*. 98, 18–28.
- Perrone, A., Lapenna, V. and Piscitelli, S. 2014. Electrical resistivity tomography technique for landslide investigation. *Earth-Science Reviews*. 135, 65-82.
- Phien-wej, N., Pientong, T. and Balasubramaniam, A.S. 1991. Collapse and strength characteristics of loess in Thailand. *Engineering Geology*. 32, 59-72.
- Rucker, M. 2006. Surface geophysics as a tool for characterization existing bridge foundation and scour conditions. *Proceedings of the Conference on Applied Geophysics*, Missouri, U.S.A., December 4-7, 2006.
- Telford, W.M., Geldart, L.P. and Sheriff, R.E. 1990. *Applied Geophysics*, Cambridge University Press, U.K.
- Tucker, S., Hurlebaus, S., Everett, M., Briaud, J.L., Medina-Cetina, Z., Yousefpour, N. and Arjwech, R. 2014. Electrical resistivity and induced polarization imaging for unknown bridge foundations. *Journal of Geotechnical and Geoenvironmental Engineering*. 141(5), 040150081-0401500811.
- Wightman, W. and Jalinoos, F. 2003. *Application Geophysical Methods to Highway Related Problem*, Federal Highway Administration, U.S. Department of Transportation, U.S.A.
- Yang, X. 1999. *Stochastic Inversion of 3D ERT Data*, Ph.D. Thesis, University of Arizona, U.S.A.